Journal of Materials Chemistry A

Accepted Manuscript

ROYAL SOCIETY OF CHEMISTRY

www.rsc.org/materialsA

Journal Name

RSCPublishing

ARTICLE

D–A–π–A featured sensitizers containing auxiliary acceptor of benzoxadiazole: molecular engineering and co-sensitization†

Cite this: DOI: 10.1039/x0xx00000x

Received 00th January 2012,
Accepted 00th January 2012

DOI: 10.1039/x0xx00000x

www.rsc.org/

Haibo Zhu,‡ Yongzhen Wu,‡ Jingchuan Liu, Weiwei Zhang, Wenjun Wu and Wei-Hong Zhu*

Two novel D-A-π-A organic sensitizers (**WS-24** and **WS-26**) incorporating a benzoxadiazole (BOD) unit are synthesized for dye sensitized solar cells. An additional *n*-hexylthiophene unit is incorporated in **WS-26** to decrease unfavourable dye aggregation, thus suppressing charge recombination and increasing the solubility. Incorporating an auxiliary acceptor of benzoxadiazole (BOD) into π-bridge can red shift absorption bands, and sharply decreases the LUMO level. In virtue of co-sensitization, the **WS-26** based DSSC device can achieve as high as 9.72% in photovoltaic efficiency.

1 Introduction

Dye sensitized solar cells (DSSCs) have attracted considerable attention due to their low cost and easy fabrication since the initial work by Grätzel's group.[1] The sensitizers play an important role and can be divided into two categories: metal complexes and metal-free organic dyes.[2] Up to now, the ruthenium–polypyridine and zinc–porphyrin based sensitizers show the champion performances, with power conversion efficiencies (PCE) around 11%~13%.[3,4] During the past decades, metal-free organic dyes usually constructed with a donor-π bridge-acceptor (D-π-A) configuration have been intensively studied owing to their lower cost, easy purification and more flexibility in molecular design.[5,6] For further improving the photovoltaic efficiency, it is necessary to extend and broaden the absorption spectra in D-π-A organic dyes. In this respect, our group has proposed a novel D-A-π-A concept for designing novel organic sensitizers which incorporate an electron-withdrawing group as auxiliary acceptor into the π bridge.[7] As demonstrated, the additional acceptor not only decreases the HOMO-LUMO energy gap, but also redistributes the charge density across the dye backbone, being capable of facilitating the photo-induced charge separation and stabilizing the electron-rich donor (such as indoline unit). A series of electron-withdrawing building blocks, such as benzothiadiazole (BTD),[8] benzotriazole (BTZ),[9] quinoxaline (QN),[10] diketopyrrolopyrrole (DPP)[11] and other units[12] have been exploited as the auxiliary acceptor. For instance, a structural engineering on the donor of quinoxaline based D-A-π-A dye (YA422) in combination with a fine device optimization leads to a high efficiency of 10.65%.[10e] A systematic study on the π-bridge of DPP based D-A-π-A dyes greatly improves the efficiency up to 10%.[11c]

In our previous study, we have found that the absorption spectra of D-A-π-A dyes can regularly shift to long wavelength when increasing the electron-withdrawing ability of auxiliary acceptor. Among the benzoheterocycle based auxiliary acceptors, BTD shows higher electron-withdrawing ability than that of BTZ and QN, thus resulting in a broader light-harvesting in BTD-based dyes. According to the knowledge from polymer science,[13] upon exchanging sulphur atom with an oxygen atom, the resulting benzoxadiazole (BOD) can induce higher electron-withdrawing ability than BTD unit. In this regard, incorporation of BOD unit in D-A-π-A based sensitizers should be preferable to the light harvesting. Moreover, compared with BTD unit, the oxygen atom in BOD is expected to have less interaction with I_2 and/or I_3^- ions than the sulphur atom, which is beneficial to retard the electron recombination.[14] However, the sensitizer containing BOD unit used in DSSCs has rarely reported.[15]

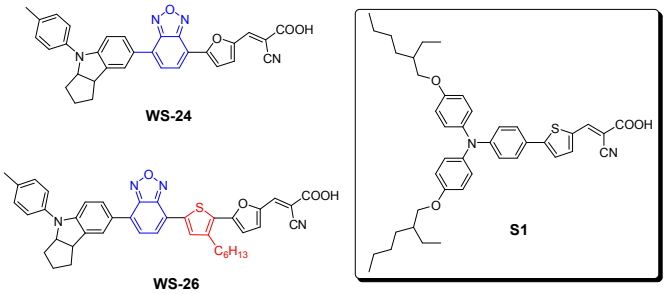

Fig. 1 Chemical structures of **WS-24**, **WS-26**, and co-sensitizer dye **S1**.

Herein we reported two BOD based D-A-π-A dyes **WS-24** and **WS-26** (Fig. 1) bearing furan as the linker, cyanoacrylic acid as the acceptor moiety and the indoline as the donor (Scheme S1 in ESI†).

One more *n*-hexylthiophene unit was incorporated in **WS-26** to decrease unfavourable dye aggregation, thus suppressing charge recombination and increasing the solubility.[16] Interestingly, **WS-26** based DSSCs exhibit a 38% increment in the power conversion efficiency (PCE) with respect to that of **WS-24**, which can be rationalized by the longer electron lifetime in the former device. Furthermore, we found that dye **WS-26** is more compatible with a known co-sensitizer **S1**[15] in a co-sensitization test.[17] After co-sensitization with **S1**, the PCE of **WS-24** based device slightly decreased from 6.21% to 5.87%, while the **WS-26** based device increased from 8.61% to 9.72%.

2 Experimental

2.1 Characterization

^{1}H and ^{13}C NMR spectra were recorded on Bruker AM 400 spectrometer with tetramethylsilane (TMS) as internal standard. HRMS were performed using a Waters LCT Premier XE spectrometer. The UV−vis spectra were measured with a Varian Cary 500 spectrophotometer. The cyclic voltammograms (CV) were determined with a Versastat II electrochemical workstation (Princeton Applied Research) using a three-electrode cell with a Pt working electrode, Pt wire counter electrode, and regular calomel reference electrode in a saturated KCl solution, 0.1 M tetrabutylammonium hexafluorophosphate ($TBAPF_6$) was used as the supporting electrolyte in DMF.

2.2 Cell device fabrication and characterizations

Photocurrent density−voltage (*I*−*V*) curves were obtained by illuminating the cell through the FTO substrate from the photoanode side under standard AM 1.5 conditions with a solar simulator (WXS-155S-10). The photocurrent action spectra were measured with a CEP-2000 system (Bunkoh-Keiki Co. Ltd.).

Electrochemical impedance spectroscopy (EIS) for DSSCs was performed using a two-electrode system under dark with electrochemical workstation (Zahner IM6e). The spectra were scanned in a frequency range of 0.1 Hz - 100 kHz at room temperature under a series of applied bias potential with a magnitude of the alternative signal of 10 mV and characterized using *Z*-View software (Solartron Analytical).

2.3 Cell Fabrication

A double-layer TiO_2 photoelectrode (a 12 μm thick nanoporous layer and a 4 mm thick scattering layer), was prepared by screen printing on conducting glass substrate following the reported procedure.[18] A dye-loaded TiO_2 electrode was dipped in the solution of dye with 3×10^{-4} M concentration in chloroform / methanol (v/v, 4/1) for 12 h, rinsed with ethanol and dried. The co-sensitized cells were prepared by immersing a TiO_2 film in the solution of **WS-24** or **WS-26** for 12 h, and then were immersed into **S1** with 3×10^{-4} M concentration in a mixture of chloroform /methanol (v/v, 4/1) for 1 h. The dye-deposited TiO_2 film and a platinum-coated conducting glass were separated by a Surlyn spacer (40 μm thick) and sealed by heating the polymer frame. In this work, 0.5 M 1-butyl-3-methylimidiazolium iodide (BMII), 0.1 M 1,2-dimethyl-3-propylimidazolium iodide (DMPII), 0.1 M LiI, 0.05 M I_2, 0.1 M guanidinium thiocyanate (GuSCN) and 0.5 M *tert*-butylpyridine (TBP) in 85/15 mixture of acetonitrile and valeronitrile were used as the redox electrolyte.

2.4 Materials and Synthesis

Bromo-substituted indoline (**a**)[19] and 4,7-dibromobenzo[*c*][1,2,5]oxadiazole (**b**)[20] were synthesized according to the established references. 4-Formylfuranboronic acid (**c**), 2-(4-hexylthiophen-2-yl)-4,4,5,5-tetramethyl-1,3,2-dioxaborolane (**d**) were purchased from *J&K* Scientific, Ltd., and used as received without further purification. THF was pre-dried over 4 Å molecular sieves and distilled under argon atmosphere from sodium benzophenone ketyl immediately prior to use. All other solvents and chemicals used in this work were of reagent grade and used without further purification.

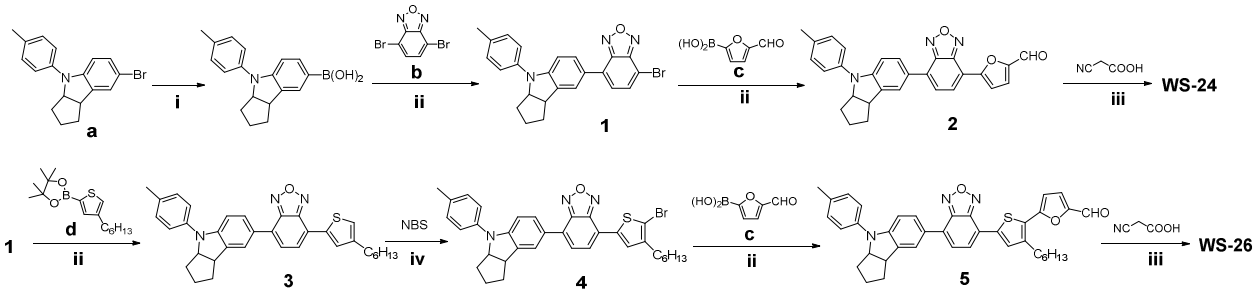

Scheme 1 Synthetic routes to **WS-24** and **WS-26**. Reagents and conditions: (i) n-BuLi, -78 °C, $B(OCH_3)_3$, THF; (ii) $Pd(PPh_3)_4$, K_2CO_3, THF; (iii) cyanoacetic acid, piperidine, acetonitrile; (iv) NBS, dichloromethane (DCM), 0 °C.

Synthesis of compound 1. To a solution of compound **a** (1.60 g, 4.87 mmol) in dry THF (30 mL) in a dried schlenk tube was added *n*-BuLi (2.4 mL, 5.76 mmol) in hexane dropwise at -78 °C, under argon in dark. After stirring for 2 h at this temperature, $B(OCH_3)_3$ (0.7 mL, 6.25 mmol) was added slowly to this solution. The reaction mixture was stirred at the same temperature for 4 h, then gradually warmed up to room temperature and used for the next Suzuki coupling reaction

without purification. In a three-neck round-bottom flask was dissolved compound **b** (1.60 g, 5.76 mmol) in THF (20 mL), a aqueous solution of 2 M K_2CO_3 (10 mL) and $Pd(PPh_3)_4$ (150 mg, 0.13 mmol) were added. After the solution was heated at 80°C, the unpurified mixture prepared above was added slowly. The reaction mixture was stirred for an additional 8 h. After cooling, water was added and the reaction mixture was extracted with CH_2Cl_2. The combined organic layer was washed with brine, dried over anhydrous Na_2SO_4, and evaporated under reduced pressure. The crude product was purified by column chromatography (CH_2Cl_2 / petroleum = 1 / 8, *V*/*V*) on silica gel to yield red powder 1.30 g, yield 59.9%. ^{1}H NMR (400 MHz, $CDCl_3$, ppm): δ 7.78 (s, 1 H), 7.72 (dd, J_1 = 8.4 Hz, J_2 = 2.0 Hz, 1 H), 7.63 (d, J = 7.5 Hz, 1 H), 7.34 (d, J = 7.5 Hz, 1 H), 7.22 (d, J = 7.1 Hz, 2 H), 7.18 (d, J = 7.1 Hz, 2 H), 6.95 (d, J = 8.4 Hz, 1 H), 4.88 (m, 1 H), 3.91 (m, 1 H), 2.35 (s, 3 H,), 2.10 (m, 1 H), 1.94 (m, 2 H), 1.79 (m, 1 H), 1.68 (m, 1 H), 1.61 (m, 1 H). ^{13}C NMR (100 MHz, $CDCl_3$, ppm): δ 150.14, 149.59, 148.91, 139.60, 135.82, 134.60, 132.37, 130.16, 129.91, 128.27, 125.41, 124.58, 124.18, 120.79, 107.38, 104.50, 69.43, 45.27, 35.32, 33.57, 24.40, 20.87. HRMS (*m*/*z*): $[M + H]^+$ calcd. for ($C_{24}H_{21}N_3O^{79}Br$), 446.0868, found 446.0866; $[M + H]^+$ calcd. for ($C_{24}H_{21}N_3O^{81}Br$), 448.0848, found 448.0847.

Synthesis of compound 2. To a 100 mL three-neck round-bottom flask was added compound **1** (300 mg, 0.67 mmol), THF (30 mL), a aqueous solution of 2 M K_2CO_3 (10 mL), 4-formylfuranboronic acid (380 mg, 2.70 mnol) and $Pd(PPh_3)_4$ (120 mg, 0.1 mmol) were added. The mixture was refluxed for 12 h under argon. After cooling, THF was removed under reduced pressure. Water was added and the reaction mixture was extracted with CH_2Cl_2. The combined organic layer was washed with brine, dried over anhydrous Na_2SO_4, and evaporated under reduced pressure. The crude product was purified by column chromatography (CH_2Cl_2 / petroleum = 1 / 1, *V*/*V*) on silica gel to yield purple red powder 158 mg, yield 51.0%. ^{1}H NMR (400 MHz, $CDCl_3$, ppm): δ 9.71 (s, 1 H), 8.08 (d, J = 7.5 Hz, 1 H), 7.89 (s, 1 H), 7.86 (dd, J_1 = 8.4 Hz, J_2 = 2.0 Hz, 1 H), 7.59 (m, 2 H,), 7.43 (d, J = 3.8 Hz, 1 H), 7.23 (d, J = 7.1 Hz, 2 H), 7.19 (d, J = 7.1 Hz, 2 H), 6.97 (d, J = 8.4 Hz, 1 H), 4.90 (m, 1 H), 3.93 (m, 1 H), 2.36 (s, 3 H), 2.11 (m, 1 H), 1.97 (m, 2 H), 1.79 (m, 1 H), 1.69 (m, 1 H), 1.60 (m, 1 H). ^{13}C NMR (100 MHz, $CDCl_3$, ppm): δ 177.27, 154.04, 152.15, 149.87, 148.97, 147.14, 139.43, 135.91, 132.56, 129.94, 128.77, 128.35, 124.76, 124.73, 124.45, 120.94, 113.97, 113.65, 107.40, 69.49, 45.25, 35.36, 33.53, 24.38, 20.88. HRMS (*m*/*z*): $[M + H]^+$ calcd. for ($C_{29}H_{24}N_3O_3$), 462.1818; found, 462.1820.

Synthesis of dye WS-24. To a 50 mL three-neck round-bottom flask was added compound **2** (150 mg, 0.33 mmol), cyanoacetic acid (280 mg, 3.3 mmol), acetonitrile (20 mL), piperidine (0.5 mL). The mixture was refluxed for 7 h under argon. After cooling, the mixture was diluted with CH_2Cl_2 (50 mL). The combined organic layer was washed with water and brine, dried over Na_2SO_4, and evaporated under reduced pressure. The crude product was purified by column chromatography (CH_2Cl_2 / MeOH = 20 / 1, *V*/*V*) on silica gel to yield the product as purple black powder 115 mg, yield 66.8%. ^{1}H NMR (400 MHz, DMSO-d_6, ppm): δ 7.90-7.98 (m, 5 H), 7.48 (d, J = 3.6 Hz, 1 H), 7.41 (d, J = 3.6 Hz, 1 H), 7.25 (d, J = 8.4 Hz, 2 H), 7.21 (d, J = 8.4 Hz, 2 H), 6.92 (d, J = 8.5 Hz, 1 H), 4.95 (m, 1 H), 3.89 (m, 1 H), 2.30 (s, 3 H), 2.01 (m, 1 H), 1.65-1.87 (m, 4 H), 1.41 (m, 1 H). ^{13}C NMR (100 MHz, DMSO-d_6, ppm): δ 162.82, 151.02, 149.44, 148.66, 148.40, 146.52, 138.94, 135.61, 133.91, 131.47, 129.82, 128.71, 127.44, 125.89, 124.40, 124.04, 121.93, 120.17, 118.43, 114.22, 113.49, 113.49, 106.80, 68.44, 44.43, 34.87, 32.93, 23.89, 20.40. HRMS (*m*/*z*): $[M + H]^+$ calcd. for ($C_{32}H_{25}N_4O_4$), 529.1876; found, 529.1874.

Synthesis of compound 3. Compound **3** was obtained as a red solid by similar procedure to that for compound **2**, but with compound **c** instead of compound **b**, 240 mg, yield 67%. ^{1}H NMR (400 MHz, $CDCl_3$, ppm): δ 7.94 (d, J = 1.1 Hz, 1 H), 7.85 (s, 1 H), 7.77 (dd, J_1 = 8.4, J_2 = 1.8 Hz, 1 H), 7.60 (d, J = 7.4 Hz, 1 H), 7.48 (d, J = 7.4 Hz, 1 H), 7.23 (d, J = 8.6 Hz, 2 H), 7.18 (d, J = 8.4 Hz, 2 H), 6.99 (s, 1 H), 6.98 (d, J = 8.7 Hz, 1 H), 4.87 (m, 1 H), 3.92 (m, 1 H), 2.68 (t, J = 7.6 Hz, 2 H), 2.35 (s, 3 H), 2.16-2.03 (m, 1 H), 2.01-1.88 (m, 2 H), 1.86-1.74 (m, 1 H), 1.74-1.63 (m, 3 H), 1.61-1.56 (m, 1 H), 1.44-1.30 (m, 6 H), 0.90 (t, J = 6.9 Hz, 3 H). ^{13}C NMR (100 MHz, $CDCl_3$, ppm): δ 149.14, 148.29, 144.91, 139.80, 137.96, 135.70, 132.11, 129.87, 129.58, 128.49, 128.07, 126.71, 125.59, 125.08, 124.57, 120.93, 120.60, 107.47, 69.38, 45.34, 35.28, 33.64, 31.70, 30.66, 30.45, 29.04, 24.42, 22.65, 20.85, 14.13. HRMS–ESI (*m*/*z*): $[M + H]^+$ calcd. for ($C_{34}H_{36}N_3OS$), 534.2579, found: 534.2579.

Synthesis of compound 4. To a 100 mL three-neck round-bottom flask was added compound **3** (220 mg, 0.41 mmol), CH_2Cl_2 (40 mL). The DCM (20 mL) solution of NBS (110 mg, 0.62 mmol) was added via a syringe at 0 °C. The mixture was stirred for 6 h under this temperature. Water was added, the organic layer was separated and removed under reduced pressure. The crude product was purified by column chromatography (CH_2Cl_2 / PE = 1 / 4) on silica gel to yield red solid 227 mg, yield 90.1%. ^{1}H NMR (400 MHz, $CDCl_3$, ppm): δ 7.84 (s, 1 H), 7.74-7.79 (m, 2 H), 7.49 (d, J = 7.4 Hz, 1 H), 7.46 (d, J = 7.4 Hz, 1 H), 7.22 (d, J = 8.6 Hz, 2 H), 7.18 (d, J = 8.5 Hz, 2 H), 6.96 (d, J = 8.4 Hz, 1 H), 4.87 (m, 1 H), 3.92 (m, 1 H), 2.62 (t, J = 7.6 Hz, 2 H), 2.35 (s, 3 H), 2.17-2.02 (m, 1 H), 2.00-1.89 (m, 2 H), 1.86-1.74 (m, 1 H), 1.73-1.62 (m, 3 H), 1.61-1.50 (m, 1 H), 1.44-1.25 (m, 6 H), 0.90 (t, J = 6.9 Hz, 3 H). ^{13}C NMR (100 MHz, $CDCl_3$, ppm): δ 149.28, 149.09, 148.01, 143.77, 139.71, 137.71, 135.74, 132.21, 129.89, 128.95, 128.92, 128.16, 126.59, 125.35, 124.90, 124.57, 120.67, 119.56, 110.41, 107.44, 69.40, 45.31, 35.29, 33.61, 31.64, 29.74, 29.70, 28.97, 24.41, 22.63, 20.86, 14.12. HRMS–ESI (*m*/*z*): $[M + H]^+$ calcd. for ($C_{34}H_{35}N_3OS^{79}Br$), 612.1684, found: 612.1686; $[M + H]^+$ calcd. for ($C_{34}H_{35}N_3OS^{81}Br$), 614.1664, found: 614.1686.

Synthesis of compound 5. Compound **5** was obtained as a red solid by similar procedure to that for compound **2**, but with compound **4** (196 mg, 0.32 mmol) instead of compound **1**, 134 mg, yield 66.7%. ^{1}H NMR (400 MHz, $CDCl_3$, ppm): δ 9.68 (s, 1 H), 8.00 (s, 1 H),

7.89 (s, 1 H), 7.83 (d, J = 8.5 Hz, 1 H), 7.67 (d, J = 7.5 Hz, 1 H), 7.54 (d, J = 7.4 Hz, 1 H), 7.37 (d, J = 3.7 Hz, 1 H), 7.25 (d, J = 8.5 Hz, 2 H), 7.21 (d, J = 8.5 Hz, 2 H), 7.00 (d, J = 8.4 Hz, 1 H), 6.72 (d, J = 8.4 Hz, 1 H), 4.91 (m, 1 H), 3.95 (m, 1 H), 2.93 (t, J = 7.7 Hz, 2 H), 2.38 (s, 3 H), 2.11-2.07 (m, 1 H), 2.09-1.90 (m, 2 H), 1.89-1.67 (m, 5 H), 1.53-1.44 (m, 2 H), 1.44-1.33 (m, 4 H), 0.93 (t, J = 6.9 Hz, 3 H). ^{13}C NMR (100 MHz, $CDCl_3$, ppm): δ 176.86, 154.48, 151.38, 149.43, 149.09, 148.12, 144.43, 139.64 138.81, 135.79, 132.31, 131.34, 129.90, 129.44, 128.31, 127.45, 125.92, 125.25, 124.80, 124.61, 120.75, 119.34, 109.24, 107.44, 69.43, 45.31, 35.31, 33.59, 31.67, 30.11, 29.92, 29.32, 24.40, 22.64, 20.86, 14.10. HRMS–ESI (m/z): $[M + H]^+$ calcd. for ($C_{39}H_{38}N_3O_3S$), 628.2634, found: 628.2634.

Synthesis of dye WS-26. Compound **WS-26** was obtained as a deep red solid by similar procedure to that for compound **WS-24**, but with compound **5** (126 mg, 0.20 mmol) instead of compound **2**,102 mg, yield 73.4%. ^{1}H NMR (400 MHz, DMSO, ppm): δ 7.96 (s, 1 H), 7.78 (s, 2 H), 7.72 (d, J = 8.4 Hz, 1 H), 7.59-7.69 (m, 2 H), 7.54 (d, J = 3.7 Hz, 1 H), 7.12-7.26 (m, 4 H), 6.94 (d, J = 3.5 Hz, 1 H), 6.84 (d, J = 8.5 Hz, 1 H), 4.83-4.93 (m, 1 H), 3.76-3.88 (m, 1 H), 2.81 (t, J = 7.3 Hz, 2 H), 2.28 (s, 3 H), 1.92-2.12 (m, 1 H), 1.67-1.87 (m, 3 H), 1.52-1.66 (m, 3 H), 1.15-1.47 (m, 7 H), 0.86 (t, J = 6.7 Hz, 3 H). ^{13}C NMR (100 MHz, DMSO, ppm): δ 163.84, 153.57, 148.31, 148.25, 147.38, 147.18, 143.86, 138.97, 137.96, 136.86, 135.42, 131.25, 130.38, 129.75, 128.11, 128.00, 127.67, 125.78, 125.72, 124.03, 123.99, 119.94, 117.75, 115.98, 111.34, 106.74, 96.75, 68.36, 44.41, 34.88, 32.92, 31.08, 29.11, 28.44, 23.91, 22.08, 20.39, 13.90. HRMS–ESI (m/z): [M^+] calcd. for ($C_{42}H_{38}N_4O_4S$), 694.2614, found: 694.2621.

3 Results and discussion

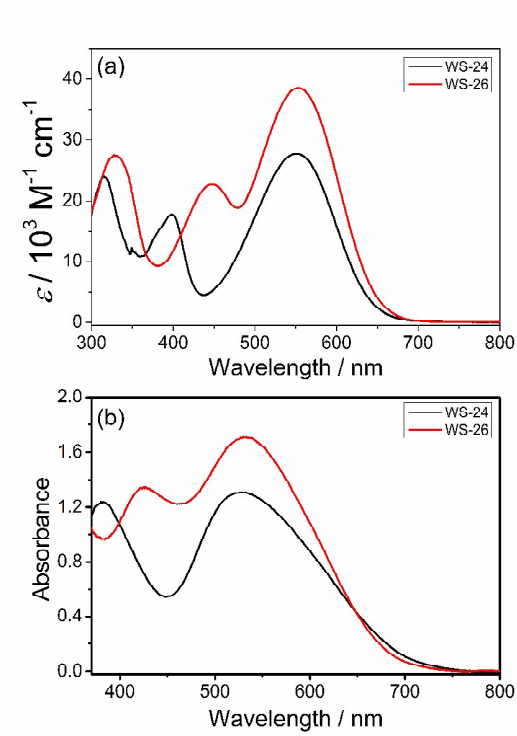

Fig. 2 Absorption spectra of **WS-24** and **WS-26**: (a) in chloroform/methanol mixed solution (v/v = 4/1) and (b) anchored on a transparent TiO_2 film.

The absorption spectra of two sensitizers in chloroform/methanol mixed solution (v/v = 4/1) and anchored on a transparent TiO_2 film are shown in Fig. 2, and the detailed parameters are summarized in Table 1. As expected, both dyes show typical absorption spectra of D-A-π-A dyes with characteristic three absorption bands in the UV region and visible region, which is different from the normal D-π-A dyes that always show two absorption bands.[7b] Although **WS-26** contains one more *n*-hexylthiophene unit in the π-conjugation, the two dyes display almost the same maximum absorption wavelength (551 nm *vs.* 552 nm) as well as threshold. The long wavelength absorption band is apparently red-shifted compared to BTD-based dye **WS-2** (533 nm)[7a] under the same conditions, which should be arisen from the stronger electron-withdrawing properties of BOD unit. The main difference in the absorption spectra of **WS-24** and **WS-26** is the middle absorption band, where the latter shows a 50 nm red shift compared to the former. This phenomenon is consistent with our previous results.[16] The two sensitizers displayed the same trend for the absorption spectra as those in solutions after anchored onto nanocrystalline TiO_2 film (Fig. 2b). They showed a hypsochromic shift of about 22 nm upon adsorption, which is probably due to the deprotonation of the cyanoacrylic acid group.[10]

Table 1 Photophysical and electrochemical properties of sensitizers **WS-24** and **WS-26**

Dyes	λ_{max}[a] (nm)	ε[a] (M^{-1} cm^{-1})	λ_{max}[b] (nm)	HOMO[c] (V)	$E_{0\text{-}0}$[d] (eV)	LUMO[e] (V)
WS-24	551	26470	528	1.01	1.79	-0.78
	398	17950				
	315	24050				
WS-26	552	38534	530	0.99	1.83	-0.84
	446	23000				
	328	27640				

Note: [a]Absorption parameters were obtained in chloroform/methanol mixed solution (v/v = 4/1). [b]Absorption parameters were obtained on 3 μm nanocrystalline TiO_2 film. [c]The HOMO was obtained in DMF with ferrocene (0.69 V vs. NHE) as external reference. [d]$E_{0\text{-}0}$ dvalues were estimated from the wavelength at 10% maximum absorption intensity for the dye-loaded 3 μm nanocrystalline TiO_2 film. [e]The LUMO was calculated according to LUMO = HOMO – $E_{0\text{-}0}$.

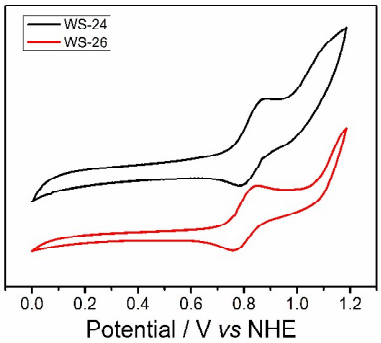

Fig. 3 Cyclic voltammograms of **WS-24** and **WS-26** in DMF solution.

To further investigate the electronic properties, their cyclic voltammetry was carried out in a typical three-electrode electrochemical cell (Fig. 3 and Table 1). **WS-24** and **WS-26** exhibit similar HOMO levels due to their same donor, calculating to be 1.01 V and 0.99 V (*vs* NHE), respectively. The driving forces for dye regeneration of **WS-24** and **WS-26** are around 0.6 eV (0.4 V *vs* NHE for I^-/I_3^- redox couple), ensuing the efficient regeneration of the oxidized dyes by I^- after electron injection.[21] Correspondingly, calculated from HOMO levels and the optical band gap, the LUMO levels of **WS-24** and **WS-26** are sharply deepened to -0.78 V and -0.84 V, respectively. Here the driving forces for electron injection from the excited dyes to the conduction band of TiO_2 (-0.5 V *vs* NHE) of **WS-24** and **WS-26** are 0.28 eV and 0.34 eV. These driving forces are theoretically enough for effective electron injection, assuming that an energy gap of 0.2 eV is indispensable for efficient electron injection.[22]

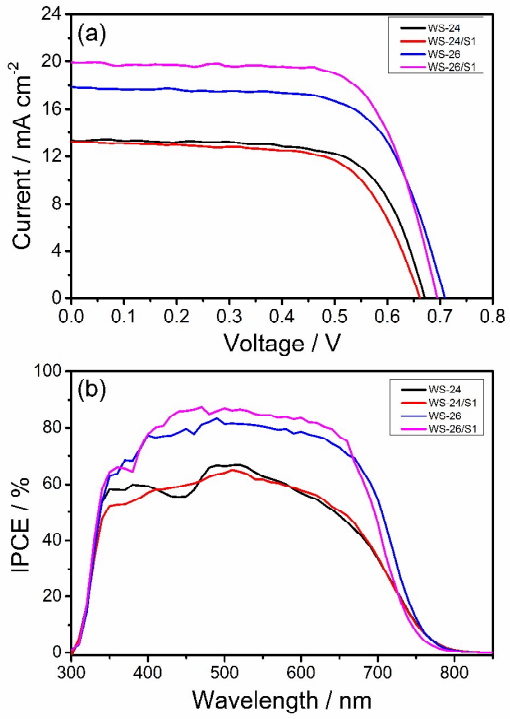

Fig. 4 (a) *J-V* curves and (b) IPCE spectra for DSSCs based on **WS-24**, **WS-26** and with the co-sensitization of **S1** under AM 1.5G simulated solar light (100 mW cm^{-2}).

Table 2 Photovoltaic parameters of DSSCs based on **WS-24**, **WS-26**, and co-sensitization with **S1**.

Dyes	J_{sc} / mA cm^{-2}	V_{oc} / mV	*FF*	η / %
WS-24	13.35±0.20	671±8	0.693±0.005	6.21±0.17
WS-24/S1	13.25±0.18	662±3	0.669±0.008	5.87±0.18
WS-26	17.84±0.24	709±6	0.681±0.011	8.61±0.32
WS-26/S1	19.84±0.38	694±8	0.706±0.006	9.72±0.39

Note: the composition of the electrolyte is: 0.5 M BMII, 0.1 M DMPII, 0.1 M LiI, 0.05 M I_2, 0.1 M GuSCN and 0.5 M TBP in 85/15 mixture of acetonitrile and valeronitrile. The parameters were obtained from the averaged five devices.

DSSCs were fabricated according to the literature.[15] The photocurrent density-voltage (*J–V*) curves of DSSCs based on **WS-24** and **WS-26** are shown in Fig. 4a, and the detailed parameters are collected in Table 2. For single dye based devices, **WS-24** show a moderate efficiency of 6.21%, with short-circuit current density (J_{sc}) of 13.35 mA cm^{-2}, open-circuit voltage (V_{oc}) of 671 mV and fill factor (FF) of 0.693. Compared to previously reported BTD based dye **WS-2** (V_{oc} = 661 mV),[16] the V_{oc} of **WS-24** is improved in spite of smaller HOMO-LUMO energy gap. The low J_{sc} of **WS-24** should be attributed to unfavourable dye aggregation. The incorporation of a hexylthiophene in **WS-26** greatly decreases the dye aggregation and improves the J_{sc} and V_{oc} to 17.84 mA cm^{-2} and 709 mV, respectively, resulting in an enhanced efficiency of 8.61%. The improvement of J_{sc} can be rationalized from the measurement of incident photon to electron conversion efficiency (IPCE) spectra as shown in Fig. 4b. Both **WS-24** and **WS-26** show a broad spectral response from 350 to 750 nm, while the plateau of **WS-26** is 20% higher than that of **WS-24**. These results suggest that a structural modification on the π-bridge of BOD based D-A-π-A dyes has significant influence on their performance in DSSCs.

Previously, we have demonstrated an effective co-sensitizer **S1** (Fig. 1) for improving the photovoltaic performance of D-A-π-A dyes. On one hand, the intensive absorption of **S1** in the blue region of solar spectrum can compensate the spectra of D-A-π-A dyes, on the other hand, **S1** plays role as co-adsorbent that suppresses the unfavourable dye aggregation on the surface of TiO_2 nanocrystallines. We also fabricated devices of **WS-24** and **WS-26** co-sensitized with **S1**. Intriguingly, we found that co-sensitized dye **S1** has a positive effect on **WS-26** and a negative effect on **WS-24**. The co-sensitization of **WS-26** with **S1** (**WS-26/S1**) improves the photovoltaic efficiency from 8.61% to 9.72%, with J_{sc} = 19.84 mA cm^{-2}, V_{oc} = 694 mV, *FF* = 0.706. The major improvement is the J_{sc}, which can be manifested by the IPCE spectra (Fig. 4b). The increase across the whole IPCE spectra and the blue-shift of the spectra threshold indicated that **S1** mainly decrease the unfavourable dye aggregation of **WS-26**. In comparison, the co-sensitization of **WS-24** with **S1** (**WS-24/S1**) gives an efficiency of 5.87%, which is almost same as the single **WS-24** based device. Apparently, the different effect of **S1** co-sensitization on dye **WS-24** and **WS-26** should be related to the π-bridge structures. The unchanged IPCE spectra of **WS-24** before and after co-sensitization with **S1** indicated that a molecular matching is crucial to the co-sensitization strategy.[23]

The V_{oc} values of **WS-26** based devices are always higher than that of **WS-24** by ~35 mV whether or not in the presence of co-sensitizers. Since all the devices employ the same electrolyte, the difference of V_{oc} should be attributed to the shift of electron Fermi level in TiO_2, which is related to the conduction band position of TiO_2 and the charge recombination rate in device.[24] The chemical structure of organic dyes on TiO_2 can affect both the energy level of TiO_2 and charge recombination resistance. To clarify the effect of π-bridge on V_{oc}, electrochemical impedance spectroscopy (EIS) measurements were performed. At a given voltage, **WS-24** and **WS-26** exhibited similar chemical capacitance, ruling out the shift of the conduction band (Fig. 5a). Thus the difference in V_{oc} should be attributed to different charge recombination rate in DSSCs, which is characterized by the electron lifetimes (τ_e). As shown in Fig. 5b, at a

fix voltage, **WS-26** showed longer electron lifetime than that of **WS-24**, suggesting that the incorporated hexylthiophene unit in the π-conjugation can reduce the contact between I_3^- in the electrolyte and the TiO_2 electrode, and thus suppressing charge recombination.

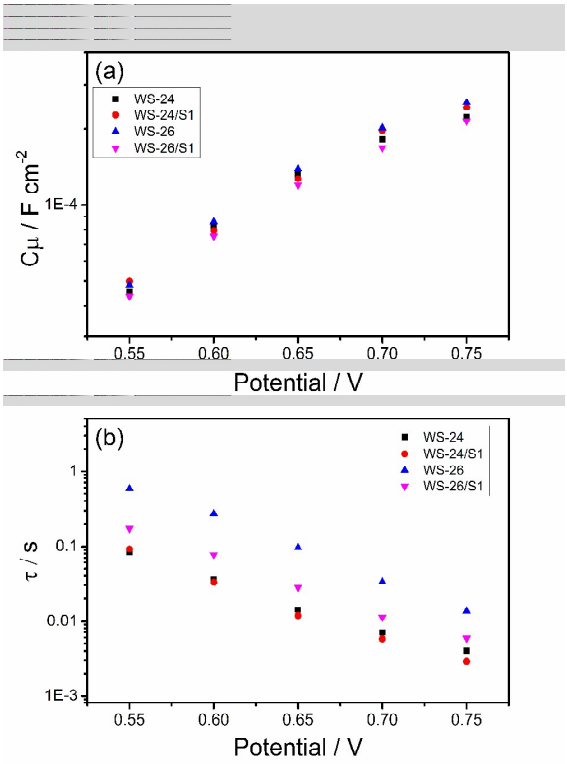

Fig. 5 TiO_2 capacitance (a) and electron lifetime (b) as a function of potential based on **WS-24**, **WS-26**, and co-sensitization with **S1**.

4 Conclusions

In summary, we have synthesized two novel BOD-based D-A-π-A organic sensitizers **WS-24** and **WS-26** for DSSCs. Compared with the well-known BTD unit, incorporating a stronger auxiliary acceptor of BOD into π-bridge can further red shift absorption bands, and predominantly deepen the LUMO orbital, especially desirable for improving light-harvesting efficiency. Although **WS-24** showed a moderate conversion efficiency of 6.21%, incorporation of a hexylthiophene unit in the π-conjugation can improve the efficiency of **WS-26** by 38.6%, achieving an efficiency of 8.61%. Interestingly, the co-sensitization with a known co-sensitizer **S1** showed negative and positive effect on dyes **WS-24** and **WS-26**, respectively. Co-sensitization of **WS-26** with **S1** (**WS-26**/**S1**) manifested an improved efficiency of 9.72%, while co-sensitization of **WS-24** with **S1** (**WS-24**/**S1**) brought forth an inferior efficiency of 5.87%. These results indicate that BOD-based D-A-π-A organic dyes are promising for developing high efficiency DSSCs, and the structure engineering as well as device optimization is crucial to enhance the photovoltaic performances.

Acknowledgements

This work was supported by NSFC for Creative Research Groups (21421004) and Distinguished Young Scholars (21325625), NSFC/China, and the Oriental Scholarship.

Notes and references

Shanghai Key Laboratory of Functional Materials Chemistry,Key Laboratory for Advanced Materials and Institute of Fine Chemicals, Collaborative Innovation Center for Coal Based Energy (i-CCE), East China University of Science and Technology, Shanghai 200237, P. R. China; E-mail: whzhu@ecust.edu.cn

‡These authors contributed equally to this work.

†Electronic Supplementary Information (ESI) available: NMR and Mass spectra. See DOI: 10.1039/b000000x/

1 B. O'Regan and M. Grätzel, *Nature*, 1991, **353**, 737.
2 (*a*) A. Hagfeldt, G. Boschloo, L. Sun, L. Kloo and H. Pettersson, *Chem. Rev.*, 2010, **110**, 6595; (*b*) S. Y. Qu, J. L. Hua and H. Tian, *Sci. China Chem.*, 2012, **55**, 677.
3 (*a*) L. Han, A. Islam, H. Chen, C. Malapaka, B. Chiranjeevi, S. Zhang, X. Yang and M. Yanagida, *Energy Environ. Sci.*, 2012, **5**, 6057; (*b*) C. Chen, M. Wang, J. Li, N. Pootrakulchote, L. Alibabaei, C. Ngoc-le, J. Decoppet, J. Tsai, C. Grätzel, C. Wu, S. M. Zakeeruddin and M. Grätzel, *ACS Nano*, 2009, **3**, 3103; (*c*) C. Chou, F. Hu, H. Yeh, H. Wu, Y. Chi, J. N. Clifford, E. Palomares, S. Liu, P. Chou and G. Lee, *Angew. Chem. Int. Ed.*, 2014, **53**, 178.
4 (*a*) A. Yella, H. Lee, H. N. Tsao, C. Yi, A. K. Chandiran, M. K. Nazeeruddin, E. W. Diau, C. Yeh, S. M. Zakeeruddin and M. Grätzel, *Science*, 2011, **334**, 629; (*b*) S. Mathew, A. Yella, P. Gao, R. Humphry-Baker, B. F. E. CurchodBasile, N. Ashari-Astani, I. Tavernelli, U. Rothlisberger, K. NazeeruddinMd. and M. Grätzel, *Nat. Chem.*, 2014, **6**, 242; (*c*) C. Wang, C. Lan, S. Hong, Y. Wang, T. Pan, C. Chang, H. Kuo, M. Kuo, E. W. Diau and C. Lin, *Energy Environ. Sci.*, 2012, **5**, 6933.
5 (*a*) A. Mishra, M. K. R. Fischer and P. Bäuerle, *Angew. Chem. Int. Ed.*, 2009, **48**, 2474; (*b*) Y. Yen, H. Chou, Y. Chen, C. Hsu and J. T. Lin, *J. Mater. Chem.*, 2012, **22**, 8734; (*c*) M. Liang and J. Chen, *Chem. Soc. Rev.*, 2013, **42**, 3453.
6 (*a*) S. Ito, S. M. Zakeeruddin, R. Humphry-Baker, P. Liska, R. Charvet, P. Comte, M. K. Nazeeruddin, P. Péchy, M. Takata, H. Miura, S. Uchida and M. Grätzel, *Adv. Mater.*, 2006, **18**, 1202; (*b*) H. Choi, I. Raabe, D. Kim, F. Teocoli, C. Kim, K. Song, J. Yum, J. Ko, M. K. Nazeeruddin and M. Grätzel, *Chem. Eur. J.*, 2010, **16**, 1193; (*c*) W. Zeng, Y. Cao, Y. Bai, Y. Wang, Y. Shi, M. Zhang, F. Wang, C. Pan and P. Wang, *Chem. Mater.*, 2010, **22**, 1915; (*d*) M. Zhang, Y. Wang, M. Xu, W. Ma, R. Li and P. Wang, *Energy Environ. Sci.*, 2013, **6**, 2944; (*e*) A. Yella, R. Humphry-Baker, B. F. E. Curchod, N. Ashari Astani, J. Teuscher, L. E. Polander, S. Mathew, J. Moser, I. Tavernelli, U. Rothlisberger, M. Grätzel, M. K. Nazeeruddin and J. Frey, *Chem. Mater.*, 2013, **25**, 2733; (*f*) R. Yeh-Yung Lin, H. Lin, Y. Yen, C. Chang, H. Chou, P. Chen, C. Hsu, Y. Chen, J. T. Lin and K. Ho, *Energy Environ. Sci.*, 2013, **6**, 2477; (*g*) X. Kang, J. Zhang, D. O Neil, A. J. Rojas, W. Chen, P. Szymanski, S. R. Marder and M. A. El-Sayed, *Chem. Mater.*, 2014, **26**, 4486; (*h*) L. Tan, J. Huang, Y. Shen, L. Xiao, J. Liu, D. Kuang and C. Su, *J. Mater. Chem. A*, 2014, **2**, 8988; (*i*) J. Liu, X. Yang, A. Islam, Y. Numata, S. Zhang, N. T. Salim, H. Chen and L. Han, *J. Mater. Chem. A*, 2013, **1**, 10889; (*g*) K. Kakiage, Y. Aoyama, T. Yano, T. Otsuka, T. Kyomen, M. Unno and M. Hanaya, *Chem. Commun.*, 2014, **50**, 6379; (*h*) W. Q. Li, B. Liu, Y. Z. Wu, S. Q. Zhu, Q. Zhang and W. H. Zhu, *Dyes Pigments*, 2013, **99**, 176.
7 (*a*) W. H. Zhu, Y. Z. Wu, S. T. Wang, W. Q. Li, X. Li, J. Chen, Z. S. Wang and H. Tian, *Adv. Funct. Mater.*, 2011, **21**, 756; (*b*) Y. Z. Wu and W. H. Zhu, *Chem. Soc. Rev.*, 2013, **42**, 2039.
8 (*a*) S. Haid, M. Marszalek, A. Mishra, M. Wielopolski, J. Teuscher, J. Moser, R. Humphry-Baker, S. M. Zakeeruddin, M. Grätzel and P. Bäuerle, *Adv. Funct. Mater.*, 2012, **22**, 1291; (*b*) D. Joly, L. Pellejà, S. Narbey, F. Oswald, J. Chiron, J. N. Clifford, E. Palomares and R. Demadrille, *Sci. Rep.*, 2014, **4**, 4033.

9 (*a*) Y. Cui, Y. Z. Wu, X. F. Lu, X. Zhang, G. Zhou, F. B. Miapeh, W. H. Zhu and Z. S. Wang, *Chem. Mater.*, 2011, **23**, 4394; (*b*) Y. Yen, C. Lee, C. Hsu, H. Chou, Y. Chen and J. T. Lin, *Chem. Asian J.*, 2013, **8**, 809.

10 (*a*) D. W. Chang, H. J. Lee, J. H. Kim, S. Y. Park, S. Park, L. Dai and J. Baek, *Org. Lett.*, 2011, **13**, 3880; (*b*) K. Pei, Y. Z. Wu, W. J. Wu, Q. Zhang, B. Q. Chen, H. Tian and W. H. Zhu, *Chem. Eur. J.*, 2012, **18**, 8190; (*c*) S. Li, C. Lee, H. Kuo, K. Ho and S. Sun, *Chem. Eur. J.*, 2012, **18**, 12085; (*d*) X. Lu, Q. Feng, T. Lan, G. Zhou and Z. Wang, *Chem. Mater.*, 2012, **24**, 3179; (*e*) J. Yang, P. Ganesan, J. Teuscher, T. Moehl, Y. J. Kim, C. Yi, P. Comte, K. Pei, T. W. Holcombe, M. K. Nazeeruddin, J. Hua, S. M. Zakeeruddin, H. Tian and M. Grätzel, *J. Am. Chem. Soc.*, 2014, **136**, 5722.

11 (*a*) S. Qu, W. Wu, J. Hua, C. Kong, Y. Long and H. Tian, *J. Phys. Chem. C*, 2010, **114**, 1343; (*b*) T. W. Holcombe, J. Yum, J. Yoon, P. Gao, M. Marszalek, D. D. Censo, K. Rakstys, M. K. Nazeeruddin and M. Grätzel, *Chem. Commun.*, 2012, **48**, 10724; (*c*) J. Yum, T. W. Holcombe, Y. Kim, K. Rakstys, T. Moehl, J. Teuscher, J. H. Delcamp, M. K. Nazeeruddin and M. Grätzel, *Sci. Rep.*, 2013, **3**, 2446.

12 (*a*) W. Q. Li, Y. Z. Wu, Q. Zhang, H. Tian and W. H. Zhu, *ACS Appl. Mater. Interfaces*, 2012, **4**, 1822; (*b*) W. Ying, F. Guo, J. Li, Q. Zhang, W. Wu, H. Tian and J. Hua, *ACS Appl. Mater. interfaces*, 2012, **4**, 4215; (*c*) J. Shi, J. Chen, Z. Chai, H. Wang, R. Tang, K. Fan, M. Wu, H. Han, J. Qin, T. Peng, Q. Li and Z. Li, *J. Mater. Chem.*, 2012, **22**, 18830; (*d*) C. Qin, A. Islam and L. Han, *J. Mater. Chem.*, 2012, **22**, 19236; (*e*) H. Li, T. M. Koh, A. Hagfeldt, M. Grätzel, S. G. Mhaisalkar and A. C. Grimsdale, *Chem. Commun.*, 2013, **49**, 2409; (*f*) Q. Feng, W. Zhang, G. Zhou and Z. Wang, *Chem. Asian J.*, 2013, **8**, 168; (g) S. Chaurasia, W. Hung, H. Chou and J. T. Lin, *Org. Lett.*, 2014, **16**, 3052.

13 (*a*) J. C. Bijleveld, M. Shahid, J. Gilot, M. M. Wienk and R. A. J. Janssen, *Adv. Funct. Mater.*, 2009, **19**, 3262; (*b*) W. Nie, R. C. Coffin, J. Liu, Y. Li, E. D. Peterson, C. M. MacNeill, R. E. Noftle and D. L. Carroll, *Appl. Phys. Lett.*, 2012, **100**, 083301; (*c*) C. V. Hoven, X. Dang, R. C. Coffin, J. Peet, T. Nguyen and G. C. Bazan, *Adv. Mater.*, 2010, **22**, E63; (*d*) H. Ting, Y. Chen, L. Lin, S. Chou, Y. Liu, H. Lin and K. Wong, *ChemSusChem*, 2014, **7**, 457.

14 (*a*) M. Tuikka, P. Hirva, K. Rissanen, J. Korppi-Tommola and M. Haukka, *Chem. Commun.*, 2011, **47**, 4499; (*b*) H. Kusama, H. Sugihara and K. Sayama, *J. Phys. Chem. C*, 2011, **115**, 2544; (*c*) H. Kusama and K. Sayama, *J. Phys. Chem. C*, 2012, **116**, 1493.

15 H. Li, Y. Z. Wu, Z. Y. Geng, J. C. Liu, D. D. Xu and W. H. Zhu, *J. Mater. Chem. A*, 2014, **2**, 14649.

16 Y. Z. Wu, M. Marszalek, S. M. Zakeeruddin, Q. Zhang, H. Tian, M. Grätzel and W. H. Zhu, *Energy Environ. Sci.*, 2012, **5**, 8261.

17 (*a*) X. Y. Youhei Numata, S. Zhang, X. Yang and L. Han, *Chem. Lett.*, 2013, **42**, 1328; (*b*) M. Cheng, X. Yang, J. Li, F. Zhang and L. Sun, *ChemSusChem*, 2013, **6**, 70.

18 S. Ito, T. N. Murakami, P. Comte, P. Liska, C. Grätzel, M. K. Nazeeruddin and M. Grätzel, *Thin Solid Films*, 2008, **516**, 4613.

19 F. S. Mancilha, B. A. D. Neto, A. S. Lopes, P. F. M. Jr., F. H. Quina, R. S. Goncalves and J. Dupont, *Eur. J. Org. Chem.*, **2006**, 4924.

20 J. C. Bijleveld, M. Shahid, J. Gilot, M. M. Wienk and R. A. J. Janssen, *Adv. Funct. Mater.*, 2009, **19**, 3262.

21 S. Wenger, P. Bouit, Q. Chen, J. Teuscher, D. D. Censo, R. Humphry-Baker, J. Moser, J. L. Delgado, N. Martín, S. M. Zakeeruddin and M. Grätzel, *J. Am. Chem. Soc.*, 2010, **132**, 5164.

22 K. Hara, T. Sato, R. Katoh, A. Furube, Y. Ohga, A. Shinpo, S. Suga, K. Sayama, H. Sugihara and H. Arakawa, *J. Phys. Chem. B*, 2003, **107**, 597.

23 G. Li, M. Liang, H. Wang, Z. Sun, L. Wang, Z. Wang and S. Xue, *Chem. Mater.*, 2013, **25**, 1713.

24 T. Marinado, K. Nonomura, J. Nissfolk, M. K. Karlsson, D. P. Hagberg, L. Sun, S. Mori and A. Hagfeldt, *Langmuir*, 2009, **26**, 2592.

Journal Name

RSCPublishing

ARTICLE

D–A–π–A featured sensitizers containing auxiliary acceptor of benzoxadiazole: molecular engineering and co-sensitization

*Haibo Zhu, Yongzhen Wu, Jingchuan Liu, Weiwei Zhang, Wenjun Wu and Wei-Hong Zhu**

Benzoxadiazole-based D–A–π–A organic sensitizers can red shift absorption bands and predominantly deepen LUMO level, realzing photovoltaic efficiency as high as 9.72% via cosensitization process.